

# Dual-Responsive Semi-Interpenetrating Network Beads Based on Calcium Alginate/Poly(*N*-isopropylacrylamide)/Poly(sodium acrylate) for Sustained Drug Release

Ximeng Sun,<sup>1,2</sup> Jun Shi,<sup>1</sup> Zhengzheng Zhang,<sup>1</sup> Shaokui Cao<sup>1</sup>

<sup>1</sup>School of Materials Science and Engineering, Zhengzhou University, Zhengzhou 450052, People's Republic of China

<sup>2</sup>Department of Chemistry, Zhengzhou University, Zhengzhou 450052, People's Republic of China

Received 5 April 2010; accepted 23 November 2010

DOI 10.1002/app.33872

Published online 5 May 2011 in Wiley Online Library (wileyonlinelibrary.com).

**ABSTRACT:** To improve the mechanical strength of natural hydrogels and to obtain a sustained drug-delivery device, temperature-/pH-sensitive hydrogel beads composed of calcium alginate (Ca-alginate) and poly(*N*-isopropylacrylamide) (PNIPAAm) were prepared in the presence of poly(sodium acrylate) (PAANa) with ultrahigh molecular weight ( $M_n \geq 1.0 \times 10^7$ ) as a strengthening agent. The influence of PAANa content on the properties, including the beads stability, swelling, and drug-release behaviors, of the hydrogels was evaluated. Scanning electron microscopy and oscillation experiments were used to analyze the structure and mechanical stability of the hydrogel beads, respectively. The results show that stability of the obtained Ca-alginate/PNIPAAm hydrogel beads strengthened by PAANa the alginate/ poly(*N*-isopropyl acrylamide)

hydrogel bead (SANBs) was significantly improved compared to that of the beads without PAANa (NANBs) at pH 7.4. The swelling behavior and drug-release capability of the SANBs were markedly dependent on the PAANa content and on the environmental temperature and pH. The bead sample with a higher percentage of PAANa exhibited a lower swelling rate and slower drug release. The drug release profiles from SANBs were further studied in simulated intestinal fluid, and the results demonstrated here suggest that SANBs could serve as a potential candidate for controlled drug delivery *in vivo*. © 2011 Wiley Periodicals, Inc. *J Appl Polym Sci* 122: 729–737, 2011

**Key words:** drug delivery systems; mechanical properties; polysaccharides

## INTRODUCTION

Temperature-/pH-responsive hydrogels are three-dimensional hydrophilic polymer networks that sharply and reversibly change their structural and physical properties in response to small variations in temperature and pH. These hydrogels are widely used in a variety of biomedical or pharmaceutical applications, particularly in the fabrication of controlled drug-delivery systems, because both temperature and pH are important environmental factors and physiological indices.<sup>1–3</sup> PNIPAAm is the best studied intelligent polymer exhibiting a thermally reversible phase transition around 32°C, called the *lower critical solution temperature* (LCST), in aqueous solution.<sup>4,5</sup> PNIPAAm can be dissolved in water below the LCST and can be precipitated from solution above the LCST. Weakly ionizable polysaccharides (e.g., alginate, chitosan, hyaluronic acid) are extensively accepted as pH-responsive hydrogels

because of their excellent biodegradability, biocompatibility, and nontoxicity.<sup>6–8</sup> Indeed, alginate gel has received increasing attention in the medical and pharmaceutical fields for its specific pH dependence. Moreover, alginate gel can be easily obtained in the presence of divalent cations, such as  $\text{Ca}^{2+}$ ,  $\text{Fe}^{2+}$ , and  $\text{Zn}^{2+}$ .

The incorporation of linear PNIPAAm into a natural hydrogel by the semi-interpenetrating network technique has been reported as an effective approach to prepare temperature/pH dual-responsive hydrogels<sup>1,2,8,9</sup> in different physical forms (e.g., membrane, column, bead) for applications as carriers to entrap and deliver drugs, proteins, and so on.<sup>3,9,10</sup> However, natural hydrogels have been found to be porous and brittle,<sup>11,12</sup> this results in a poor mechanical strength. The integration of a synthetic hydrophilic polymer, such as poly(vinyl alcohol), poly(ethylene glycol), or poly(acrylic acid), into natural hydrogel matrices is one possible strategy<sup>13–18</sup> for improving the mechanical strength of natural hydrogels. Blend films and beads consisting of poly(vinyl alcohol) and alginate or chitosan have recently been developed,<sup>13–15</sup> and the resulting hydrogels combined the appropriate mechanical properties of the synthetic component with the biocompatibility of the biological component. On the other hand, PAANa with ultrahigh molecular weight ( $M_n > 1.0 \times 10^7$ ) is extensively accepted as an excellent food additive and

Correspondence to: S. K. Cao (caoshaokui@zzu.edu.cn) and J. Shi (shijun@zzu.edu.cn).

Contract grant sponsor: National Natural Science Foundation of China; contract grant number: 20874090.

has been used to improve the flexibility and toughness of food in the food industry and has been used as a thickening or stabilizing agent in the formulation of pharmaceutical emulsions and suspensions.<sup>19–21</sup> The mechanism for the function of PAANa is due to the physical entanglement interaction between the long chains of PAANa and the starch or cellulose molecules in food. Similarly, it should be reasonable to improve the mechanical strength of alginate gel through the introduction of PAANa, and related research is rarely found in the literature.

In our previous studies,<sup>10,22</sup> we found that temperature-/pH-responsive Ca-alginate/PNIPAAm hydrogel beads used as drug carriers were easily broken in phosphate buffer solution (PBS) at pH 7.4, which resulted in relatively quick swelling and drug release. Hence, as a part of our continuous research, PAANa with ultrahigh molecular weight was introduced to prepare Ca-alginate/PNIPAAm/PAANa hydrogel beads. The aim of this study was to make full use of the physical entanglement interaction between the long chains of PAANa and alginate to improve the mechanical stability and sustained drug release of non-strengthened alginate/poly(N-isopropyl acrylamide) bead (NANBs). The mechanical stability, swelling, and drug-release behaviors of the alginate/poly(N-isopropyl acrylamide) hydrogel bead (SANBs) were investigated comparatively with NANBs in PBS at pH 7.4 and HCl solution at pH 1.2 (which are similar to the pH values of intestinal and gastric fluids, respectively) at different temperatures.

## EXPERIMENTAL

### Materials

N-Isopropylacrylamide (NIPAAm) was purchased from Tokyo Chemical Industry Co., Ltd. (Tokyo, Japan). Na-alginate (20 cps, viscosity = 1.0% solution at 20°C), ammonium persulfate (APS), and *N,N,N,N*-tetramethylethylenediamine (TEMED) were all obtained from Shanghai Chemical Reagent Co., Ltd. (Shanghai, China). PAANa with ultrahigh molecular weight ( $M_n \approx 1.0 \times 10^7$ ,  $2.0 \times 10^7$ , and  $3.0 \times 10^7$ ) was provided by Henan Kai-Te Chemical Industry General Co. (Henan, China), and indomethacin (IDMC) was obtained from Shanghai Hou-Cheng Fine Chemical Co., Ltd. (Shanghai, China). All other chemicals were commercially products with analytical purity.

### Synthesis of PNIPAAm

Linear PNIPAAm was synthesized by the free-radical polymerization of NIPAAm monomer with APS as an initiator in the presence of TEMED, as previously described.<sup>10,23</sup> NIPAAm (35.3 mmol) was dissolved in 45 mL of deionized water, followed by the

addition of APS (0.53 mmol); then, nitrogen was bubbled through the solution for 30 min to exclude oxygen. TEMED (0.267 mmol) was then added. The polymerization was carried out at room temperature for 8 h. The product, PNIPAAm, was isolated and purified repeatedly by precipitation in hot water and dissolution in cool water and finally dried *in vacuo* at 40°C for 48 h.

### Preparation of NANBs and SANBs

To prepare NANBs, PNIPAAm was dissolved in a 1.5% (w/v) aqueous solution of Na-alginate, the mass ratio of PNIPAAm to Na-alginate was 1 : 3, and then, IDMC (20 wt %, relative to the total weight of Na-alginate and PNIPAAm) and NaCl (0.9%, w/v) were added and dispersed homogeneously. The mixed solution was extruded dropwise with a syringe needle into a 3% (w/v) aqueous solution of  $\text{CaCl}_2$  under gentle stirring. The spherical beads that formed were kept in a  $\text{CaCl}_2$  solution for 40 min to make the beads completely crosslink; this was followed by three washings with deionized water to remove the unattached drug from the bead surface. Finally, the resultant beads were air-dried overnight and then vacuum-dried at 40°C for 24 h.

The preparation procedure for SANBs was similar to that for NANBs. The only difference was that the ultrahigh-molecular-weight PAANa was dissolved into the mixed solution of Na-alginate and PNIPAAm. The total concentrations of PAANa in the mixed solution were 0.05 and 0.1% (w/v) for the bead samples SANB-1 and SANB-2, respectively.

### Characterization and property measurements

#### Fourier transform infrared (FTIR) spectroscopy

The FTIR spectra of the sample beads and pure IDMC were recorded on a Nicolet spectrophotometer (Nicolet Nexus 470, Wisconsin, USA) in the range 500–4000  $\text{cm}^{-1}$  with KBr pellets.

#### Differential scanning calorimetry (DSC) measurements

DSC curves were recorded to determine the LCST of the sample beads with a differential scanning calorimeter (Netzsch 204, Selb, Germany). The analysis was performed from 0 to 45°C at a heating rate of 5°C/min and under a nitrogen flow of 20  $\text{cm}^3/\text{min}$ .

#### Morphological characterization

The external and internal morphologies of the dried beads were studied with scanning electron microscopy (SEM; FEI Quanta 200, FEI Co., Holland) at an accelerated voltage of 20 kV. Before the observation, the beads were stabilized on aluminum stubs with

adhesive and were sputter-coated with an approximate 100-Å layer of gold with a vacuum evaporator.

### Swelling measurements

The swelling behaviors were determined gravimetrically. The prepared dried beads were accurately weighed and then immersed into conical flasks containing 30 mL of PBS at pH 7.4 and HCl solution at pH 1.2 at 25, 37, and 45°C, respectively. Periodically, the beads were taken out and weighed after the excess surface water was absorbed with moistened filter paper. This procedure was continued until the weight of beads was kept constant or reached a maximum value. The swelling degrees at random time ( $SD_t$ ), at the swelling equilibrium state ( $SD_{eq}$ ), and at the maximum swelling state ( $SD_{max}$ ) and the swelling rate ( $k$ ;  $\text{min}^{-1}$ ) were calculated from the following relations:<sup>24</sup>

$$SD_t = \frac{w_t - w_0}{w_0}, \quad SD_{max} = \frac{w_{max} - w_0}{w_0},$$

$$SD_{eq} = \frac{w_{eq} - w_0}{w_0}, \quad kt = -\ln(w_{eq} - w_t)$$

where  $t$  is the time (min),  $w_0$  is the initial bead weight (g) in the dry state,  $w_t$  is the bead weight (g) at time  $t$ ,  $w_{max}$  is the bead weight (g) at the maximum swelling state, and  $w_{eq}$  is the bead weight at the swelling equilibrium state, respectively. Each experiment was repeated for three times.

### In vitro drug release

**Determination of drug loading.** Drug loading of the studied beads was estimated according to the previously reported method.<sup>25,26</sup> The accurately weighed beads were immersed into 100 mL of PBS (containing 5.0 mL of ethanol) and then were stirred for over 24 h to be broken completely. The absorbance of the clear supernatant solution was measured by an ultraviolet-visible spectrophotometer (Shimadzu, Japan) at an  $\lambda_{max}$  value of 320 nm for IDMC. Quantitative drug loading was obtained by comparison with the IDMC standard curve. The drug loading was calculated from the following equation:

$$\text{Drug loading (mg/g)} = \frac{\text{Concentration of the drug (mg/mL)} \times 100 \text{ (mL)}}{\text{Weight of the beads (g)}}$$

### Cumulative drug release

*In vitro* drug release experiments were carried out with a horizontal laboratory shaker at 25, 37 and 45°C, respectively. Accurate quantities of the dry

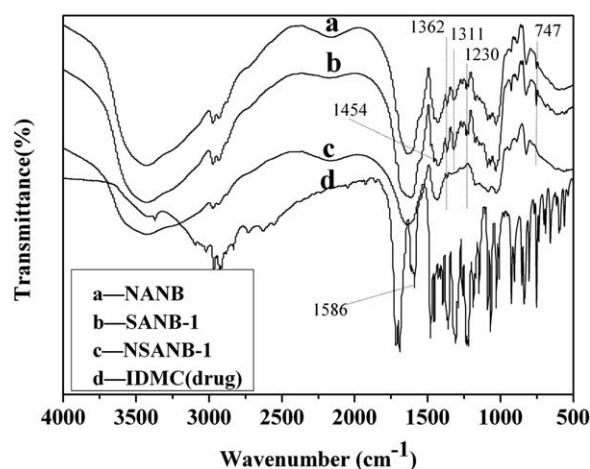


**Figure 1** FTIR spectra of (a) NANB, (b) SANB-1, (c) plain SANB-1, and (d) pure IDMC drug.

beads (0.0100 g) was immersed into conical flasks containing 50 mL of PBS (pH 7.4) and 50 mL of HCl solution (pH 1.2) with shaking at 50 rpm. A 2-mL aliquot of release medium was periodically taken out, and the IDMC concentration in each aliquot was measured with an ultraviolet-visible spectrophotometer at 320 nm, and the amount of released drug was obtained by comparison with the calibration curve. A 2-mL aliquot of fresh PBS was added back to the conical flask to keep the total volume constant. All drug-release studies were performed in triplicate, whereas only the average values are shown in the data analysis.

### Statistical analysis

A Student's  $t$  test was used to determine the differences between the results. A value of  $p < 0.05$  was considered statistically significant.

## RESULTS AND DISCUSSION

### Characterization of the bead samples

Figure 1 presents the FTIR spectra of NANB, SANB-1, SANB-1 without drug (plain SANB-1), and pure IDMC. It was clear that there was no obvious difference between NANB and SANB-1, whereas significant differences were observed between SANB-1 and plain SANB-1. When IDMC was incorporated into SANB-1, along with all of the almost same characteristic peaks of the plain SANB-1, additional bands appeared due to the presence of IDMC in the matrix. For instance, SANB-1 showed characteristic bands at 1695 and 1586  $\text{cm}^{-1}$ , which were ascribed to the  $\nu(\text{C}=\text{O})$  and  $\nu(\text{C}-\text{N})$  modes of  $-\text{HN}-\text{CO}-$  in IDMC. The band at 1454  $\text{cm}^{-1}$  was due to the  $\nu(\text{C}-\text{C})$  stretching modes of the aromatic rings, and the characteristic band around 747  $\text{cm}^{-1}$  was due to

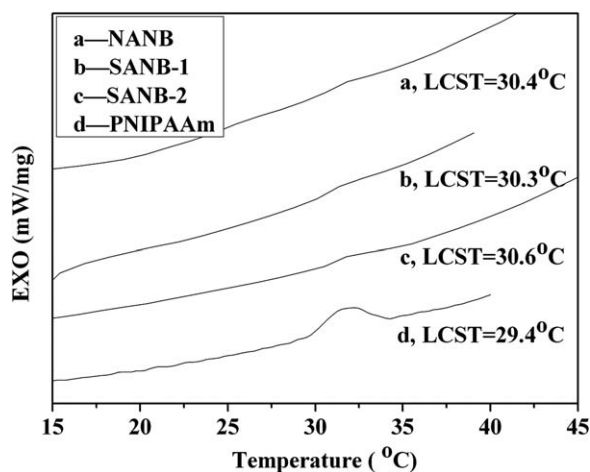


**Figure 2** DSC thermograms of (a) NANB, (b) SANB-1, (c) SANB-2, and (d) PNIPAAm.

aromatic C—Cl stretching in IDMC.<sup>27</sup> This also indicated that IDMC did not have any chemical changes after being incorporated into the beads.

The LCSTs of NANB, SANB-1, SANB-2, and PNIPAAm were determined by DSC measurements. The values of the onset temperature of the peaks (defined as LCST) are presented in Figure 2. Only a slight difference could be found among the three samples with increasing PAANA content, and their LCSTs were almost equal to that of PNIPAAm.

The morphology of NANB and SANB-1 was illustrated by the SEM micrographs in Figure 3. To gain clear insight into the surface morphology, the micrographs were recorded with two different magnifications, as shown [Fig. 3(a,b), 100 $\times$ ; Fig. 3(c,d), 500 $\times$ ]. These images indicate that both NANB and SANB-1 appeared almost spherical in shape, whereas NANB showed a rougher surface with larger wrinkles. Figure 3(e,f) (500 $\times$ ) shows the cross-section morphology, in which NANB showed some obvious big cracks and pores, whereas SANB-1 did not. In other words, the internal structure of SANB-1 was more compact than that of NANB because of the introduction of a small amount of PAANA.

### Stability assessment

All of the bead samples were exposed to both oscillation and osmotic swelling pressure to evaluate the mechanical stability in PBS (pH 7.4) under oscillation (50 rpm).<sup>28,29</sup> Figure 4 shows three digital photographs, where the shapes of sample beads in each cylinder can be observed. Only NANBs ruptured after 4 h at 45 $^{\circ}$ C, 12 h at 37 $^{\circ}$ C, and 48 h at 25 $^{\circ}$ C; this indicated that SANB-1 and SANB-2 provided higher mechanical resistance, even with a small amount of PAANA. The possible reason was that the PAANA long chains could penetrate into the Ca-alginate gel, and then, the strong entanglement interactions could

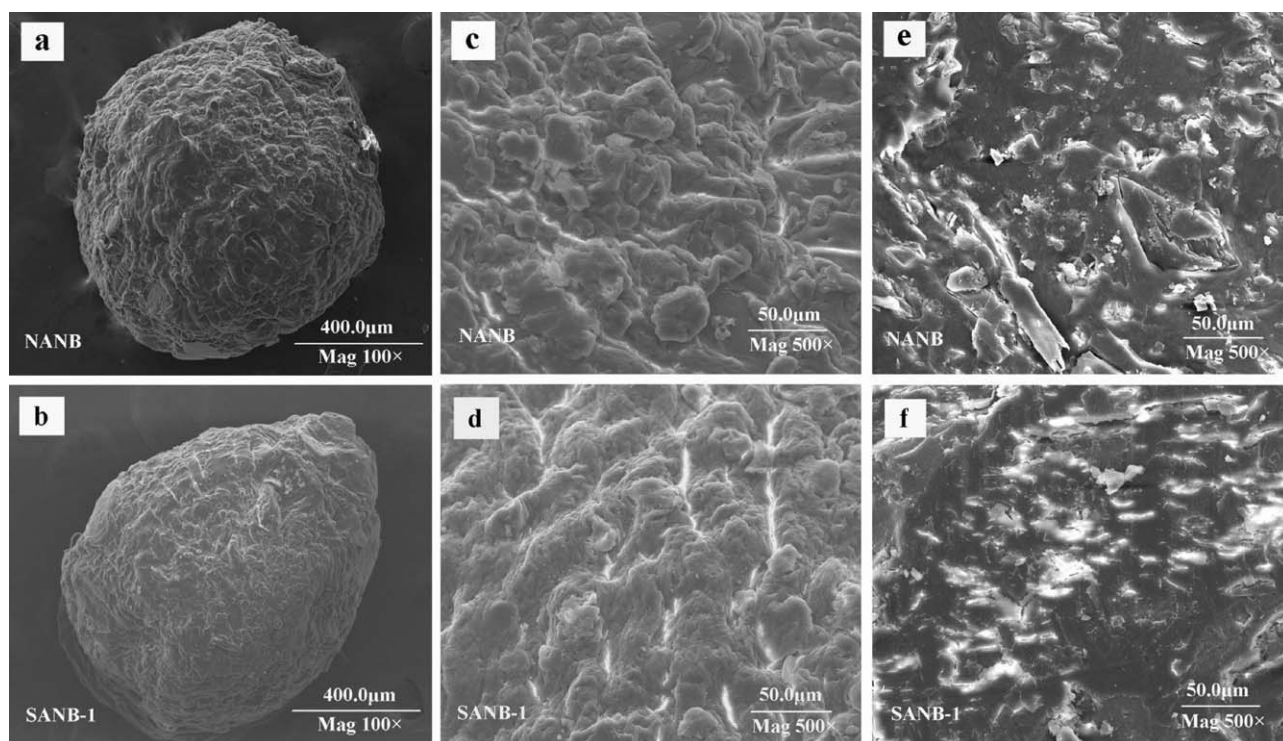


**Figure 3** SEM micrographs of NANB and SANB-1: (a,b) surface morphology (100 $\times$ ), (c,d) surface morphology (500 $\times$ ), and (e,f) cross-section morphology (500 $\times$ ).

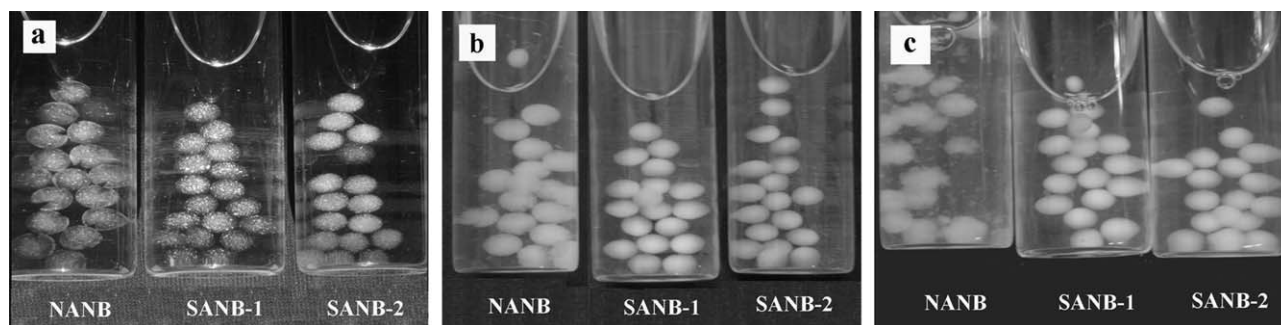


**Figure 4** Digital photographs of the studied hydrogel beads at pH 7.4: (a) at 25°C for 60 h, (b) at 37°C for 12 h, and (c) at 45°C for 4 h.

be formed between the PAANa long chains and the Ca-alginate gel networks. These entanglement interactions inhibited the breakage of Ca-alginate gel, and as a result, SANBs showed better flexibility and stronger stability than NANBs.

#### Temperature/pH-sensitive swelling

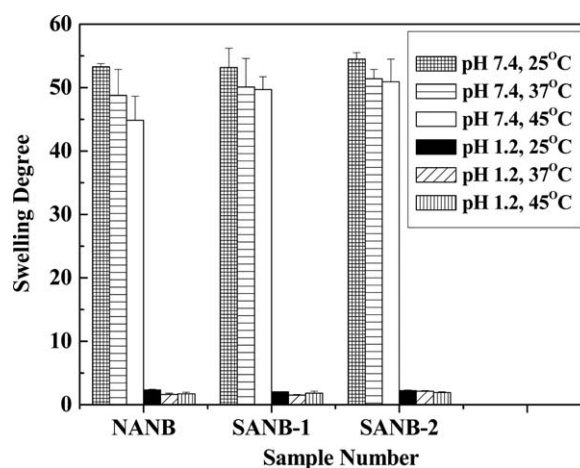
Figure 5 shows swelling behaviors of NANB, SANB-1, and SANB-2 at different pH values and temperatures. The  $SD_{eq}$  (or  $SD_{max}$ ) of the studied beads at pH 7.4 was much higher than that at pH 1.2. This was mainly attributed to the carboxylic acid groups linked on the Ca-alginate gel. At pH 1.2, most of the carboxylic groups in the Ca-alginate gel should have existed in the form of  $-COOH$ , as the  $pK_a$  of alginate was about 3.2 to 4.0.<sup>2,6,15</sup> The hydrogen bonds between  $-COOH$  in Ca-alginate gel and  $-CONH-$  in PNIPAAm led to the polymer-polymer interactions, which predominated over the polymer-water interactions. Therefore, the beads shrank and hardly swelled. Once the beads were immersed in PBS at pH 7.4, the carboxylic groups in Ca-alginate gel became ionized and existed in the form of  $-COO^-$  anion. The electrostatic repulsion between  $-COO^-$  caused the hydrogel to swell. Meanwhile, the hydrogen bonds between  $-COO^-$  and  $H_2O$  were easily formed, and then, the beads absorbed water and swelled. The analysis of a Student's  $t$  test showed that the differences between the  $SD_{eq}$  of all of the studied beads were statistically significant (>95% confidence interval) at both pH 7.4 and 1.2, and the  $p$  values were about 0.0001. Therefore, we concluded that the  $SD_{eq}$  values of all of the samples were higher at pH 7.4 than at pH 1.2.

Figure 5 also indicates that  $SD_{eq}$  (or  $SD_{max}$ ) tended to decrease at pH 7.4 with increasing temperature for all bead samples. For example,  $SD_{eq}$  of SANB-1 reached 55.5 at 25°C, 50.9 at 37°C, and 50.1 at 45°C, respectively. The analysis of a Student's  $t$  test showed that the differences between the sample's  $SD_{eq}$  (or  $SD_{max}$ ) under different temperatures were statistically significant, and the  $p$  values were in the

range 0.0285–0.0460. This phenomenon resulted from the shrinkage of PNIPAAm chains penetrating into the Ca-alginate gel when the temperature was above the LCST of PNIPAAm. The  $SD_{eq}$  values of both SANB-1 and SANB-2 were slightly higher than that of NANB at pH 7.4 under the corresponding temperature, which might have been due to the introduction of PAANa, which increased the toughness and strength of the SANBs. However, the differences between the  $SD_{eq}$  values of SANB-1 and SANB-2 were not statistically significant ( $0.783 > p > 0.1668$ ).

#### Swelling kinetics

The swelling kinetics of all of the studied beads samples were investigated by swelling experiments in PBS at pH 7.4. Figure 6(a) shows the time-dependent swelling profiles of the beads at 25, 37, and 45°C, respectively. It was found that the  $SD_t$  values of all of the samples increased with prolonged time until their  $SD_t$  tended to the  $SD_{max}$ , whereas the  $SD_t$  of SANB-1 was similar to that of SANB-2 ( $p > 0.188$ ), and the  $SD_t$  values of both SANB-1 and SANB-2 were obviously lower than that of NANB at the same time intervals before  $SD_{max}$  ( $0.034 > p >$



**Figure 5** Temperature- and pH-dependent changes of  $SD_{eq}$  for the studied beads.

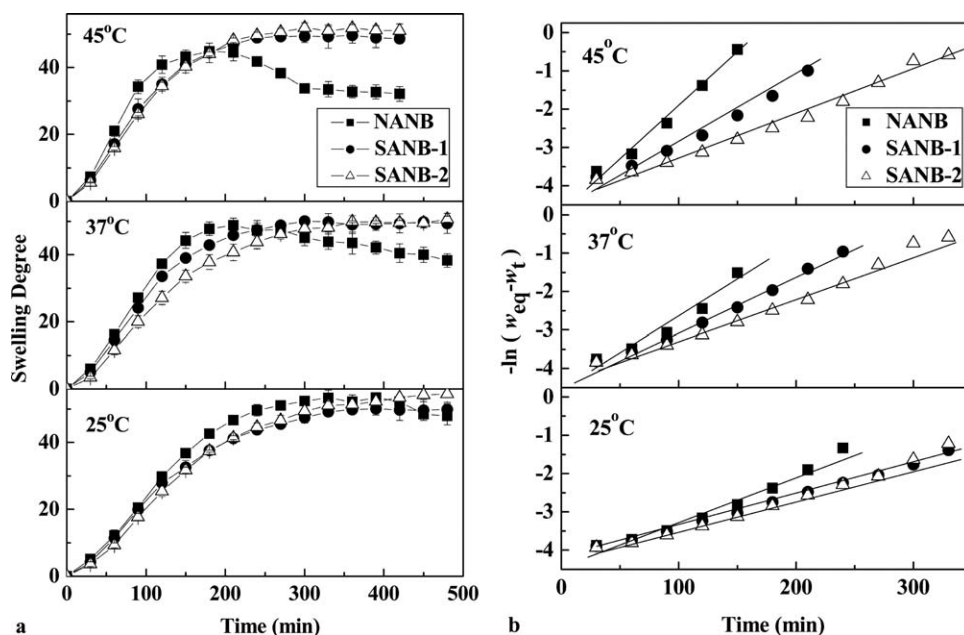


**Figure 6** (a) Swelling degree and (b) swelling rate ( $k$ ;  $\text{min}^{-1}$ ) of the studied beads at pH 7.4 measured at 25, 37, and 45°C.

0.0001). After  $SD_{\max}$ , the  $SD_t$  values of SANB-1 and SANB-2 tended to be a constant value called  $SD_{\text{eq}}$ , whereas the  $SD_t$  of NANB decreased gradually. The differences in the swelling behaviors came from their different structures and strengths caused by PAANA. For SANBs, the strong entanglement interactions formed between the long chains of PAANA and the Ca-alginate gel networks slowed the extension of the hydrogel network and inhibited the breakage of the Ca-alginate gel.

The swelling rate ( $k$ ;  $\text{min}^{-1}$ ) of the studied beads before  $SD_{\text{eq}}$  (or  $SD_{\max}$ ) is shown in Figure 6(b). The swelling rate of the beads decreased with the increase of PAANA content at 37 and 45°C, whereas the swelling rate of SANB-1 was similar to that of SANB-2 at 25°C. For example, the swelling rate was about  $0.0194 \text{ min}^{-1}$  for NANB,  $0.0143 \text{ min}^{-1}$  for SANB-1, and  $0.0103 \text{ min}^{-1}$  for SANB-2 at 37°C. The swelling kinetics of all of the studied beads was formally described as a first-order chemical reaction. This phenomenon indicates that the swelling rate of SANBs was limited because of the presence of PAANA. For SANBs, the PAANA long chains could penetrate randomly into the Ca-alginate gel networks, and the strong entanglement interactions between PAANA and the hydrogel networks were formed, and then, the mechanical strength of SANB was obviously enhanced in comparison with that of the NANBs. As a result, the swelling rate of the SANBs became lower than that of the NANBs. It is also shown in Figure 6(b) that the swelling rate of the hydrogel beads increased gradually with increasing temperature. A possible explanation is that PNI-

PAAm chains shrank above LCST, and therefore, the gel pore radius became enlarged. Another explanation is that water molecules would gain enthalpy at higher temperatures. Consequently, these two factors accelerated water to penetrate quickly into the beads, as reported in previous literature.<sup>30</sup>

### *In vitro* drug release

#### Effect of PAANA introduction

For temperature-/pH-responsive controlled drug-delivery systems, drug will be released first by the diffusion mechanism and then by the degradation mechanism. NANBs are easily broken in PBS at pH 7.4, and therefore, their swelling and drug-release rates are high. To obtain lower release rates of drugs, PAANA was introduced into the Ca-alginate/PNIPAAm hydrogel to enhance the mechanical strength and slow the drug release. Figure 7 shows the IDMC release profiles from the prepared beads in PBS at 25°C [Fig. 7(a)] and 37°C [Fig. 7(b)]. The results reveal that the IDMC release from both SANB-1 and SANB-2 was obviously lower than that from NANB at both 25 and 37°C. Analysis of Student's  $t$  test showed that the differences between these results were statistically significant, and the obtained  $p$  values in comparison with the data from NANB and SANB-1 or SANB-2 were in the range 0.0001–0.0004 for the total time period of 60–480 min. The amount of released IDMC was about 76.1% for SANB-1 and 65.2% for SANB-2, respectively. The IDMC release reached 98.3% for NANB within the first 300 min at 37°C. Meanwhile, the

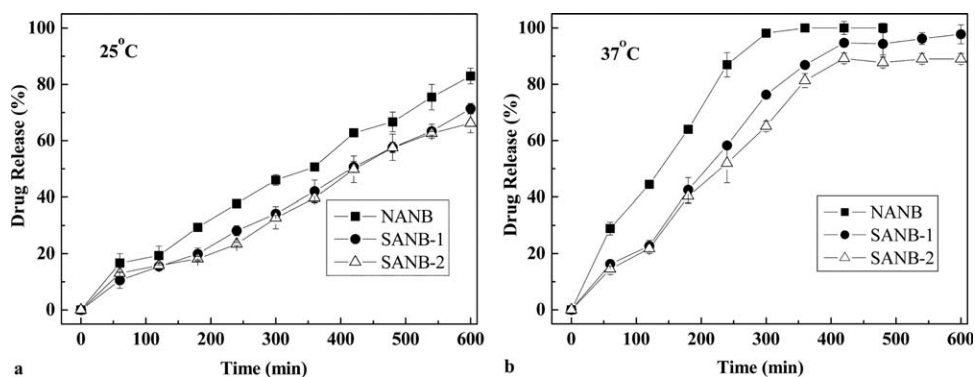


Figure 7 Effect of PAANa on IDMC release at pH 7.4 measured at 25 and 37°C.

released amount of IDMC showed a tendency to decrease with increasing PAANa content at 37°C, but the differences between the drug release from SANB-1 and SANB-2 was narrow. This phenomenon might have been due to the strong physical entanglement interactions between the PAANa long chains and the Ca-alginate gel networks. As a result, the interior structure of SANBs became more compact, and their toughness, flexibility, and strength could be greatly improved. Consistently, the release rate of IDMC from both SANB-1 and SANB-2 was slower than that from NANB.

It is worth noting that bead samples strengthened by the same amount of different molecular weight PAANa's (e.g.,  $M_n \approx 2.0 \times 10^7$  and  $3.0 \times 10^7$ ) were prepared. Their drug-release profiles were similar to that of SANB-1, and therefore, their drug-release behaviors are not discussed in this article.

#### Effect of pH

SANB-1 was optimized to investigate the effect of pH value on the drug release. Figure 8 presents the drug-release profiles at 37°C from SANB-1 at pH 1.2 and 7.4. Significant pH-dependent release profiles were observed. The cumulative IDMC release at pH 7.4 was much higher than that at pH 1.2. The amount of released IDMC was about 90% within 420 min at pH 7.4, whereas it was only 15% at pH 1.2. A Student's *t*-test analysis showed that the differences between the data of released IDMC at pH 7.4 and 1.2 were statistically significant during the referred time period ( $0.002 > p > 0.0008$ ). This release behavior was closely related to the swelling behavior of SANB-1, as shown in Figure 6. In PBS at pH 7.4, the volume of SANB-1 increased gradually, and the pore sizes became enlarged; therefore, the external medium could diffuse into the hydrogel beads quickly, and the drug could be dissolved and released because of the osmotic pressure. However, SANB-1 scarcely swelled, and the pore sizes were very small at pH 1.2. Therefore, the amount of

released drug was much lower than that at pH 7.4. As a result, SANB-1 could bypass the acidic gastric fluid without liberating the loaded drug when it was used as the oral drug carrier.

#### Effect of the temperature

Figure 9 shows the IDMC release profiles from SANB-1 in PBS of pH 7.4 at 25, 37, and 45°C. A temperature-dependent response was observed. The release rates of IDMC at both 37 and 45°C were much higher than that at 25°C. The cumulative amount of released IDMC reached 90% within 480 min at 37°C, whereas the value was only 68% at 25°C within 720 min. The differences between the data of released drug from SANB-1 at 25 and 37 or 45°C were found to be statistically significant, and the *p* values were in the range 0.0001–0.031 within 600 min. In addition, the *p* values between the drug release at 37 and 45°C were from 0.0001 to 0.0079 for the time period between 60 and 420 min; this indicated that the differences in the data of released drug at 37 and 45°C were also statistically significant. There were three possibilities to explain this phenomenon. First, PNIPAAm chains spread and

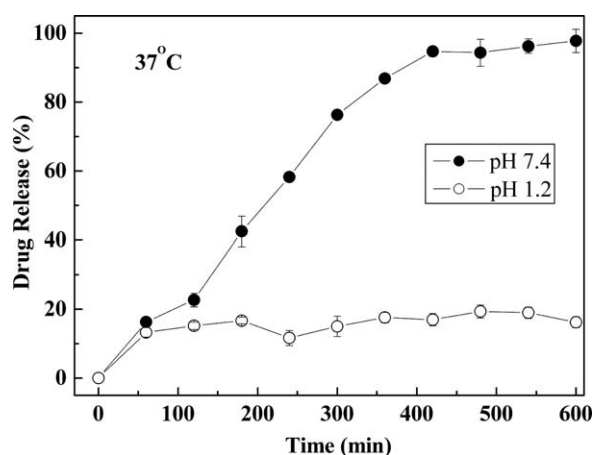
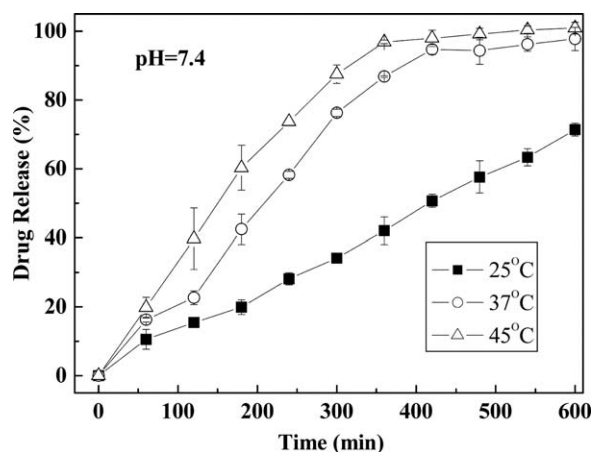


Figure 8 pH-dependent release profiles of IDMC at 37°C from SANB-1 measured at pH 1.2 and 7.4.



**Figure 9** Temperature-dependent release profiles of IDM from SANB-1 measured at pH 7.4.

distributed randomly in the hydrogel network at 25°C, whereas they became more hydrophobic and collapsed at temperatures above 37°C, and therefore, the gel pore sizes became enlarged.<sup>31,32</sup> This could have accelerated the external PBS to diffuse into the beads, and then, the drug release would have increased. Second, the entrapped drug molecules were squeezed out through the enlarged pores because of the collapsing of hydrogel network at 37 or 45°C. Finally, the disruption of the Ca-alginate gel was apt to occur in PBS at pH 7.4.

### Drug-release kinetics

We analyzed the drug-release kinetics by plotting the cumulative release data versus time by fitting them to the following empirical equation:<sup>33,34</sup>

$$\frac{M_t}{M_\infty} = kt^n$$

where  $M_t$  and  $M_\infty$  are the cumulative amounts of IDM released at time  $t$  and equilibrium time, respectively;  $k$  is a kinetic constant relating to the hydrogel system; and  $n$  is the diffusional exponent, which suggests the nature of the release mechanism.  $n$  values are determined from the slope of the plot of  $\ln(M_t/M_\infty)$  versus  $\ln t$ . A value of  $n = 0.5$  indicates Fickian diffusion (case I transport), whereas polymer chain relaxation becomes the rate-controlling factor for case II transport (relaxation controlled) if  $n = 1.0$ . When the value of  $n$  is between 0.5 and 1.0, the release follows anomalous or non-Fickian diffusion, where the system will be diffusion- and relaxation-controlled.

In this research, the  $n$  values in Figure 10 showed a dependence on PAANA for NANB and SANB-1. The  $n$  values of NANB ranged from 0.436 to 0.750 and produced a shift from Fickian diffusion to

anomalous transport. As for SANB-1, a model S-shaped curve was observed. The S curve could be divided into three regions: the diffusion exponents corresponding to these stages were  $n_3$ ,  $n_4$ , and  $n_5$ , respectively. The  $n_3$  value ( $n_3 = 0.053$ ) indicated that Fickian diffusion was the prominent transport mechanism at the beginning of the release process. The  $n_4$  value ( $n_4 = 1.098$ ) indicated that relaxation-controlled transport played an important role in the subsequent stage. In the last stage, the Fickian diffusion mechanism became dominant, which, again, was revealed by the  $n_5$  values ( $n_5 = 0.558$ ). These observations were in line with the swelling study.

### CONCLUSIONS

We successfully combined natural Ca-alginate gel, PNIPAAm, and PAANA with ultrahigh molecular weight ( $M_n \geq 1.0 \times 10^7$ ) to produce new strengthened temperature-/pH-sensitive hydrogel beads, which could be used as drug-delivery devices for IDM. The mechanical stability, surface and interior morphologies, and swelling and drug-release behaviors of the obtained beads were investigated. It was clearly demonstrated that all of the mentioned properties were affected by the introduction of PAANA in PBS at pH 7.4. Both SANB-1 and SANB-2 with only a little of PAANA showed a much improved mechanical strength and a more compact surface and interior morphologies compared with NANB. The swelling and drug-release experiments clearly revealed that the swelling and drug-release behaviors were significantly dependent on the PAANA content and on the environmental temperature and pH. Drug release from SANBs was found to be retarded, and the swelling rate of SANBs became lower than that of NANBs under neutral conditions. These improved properties by PAANA introduction

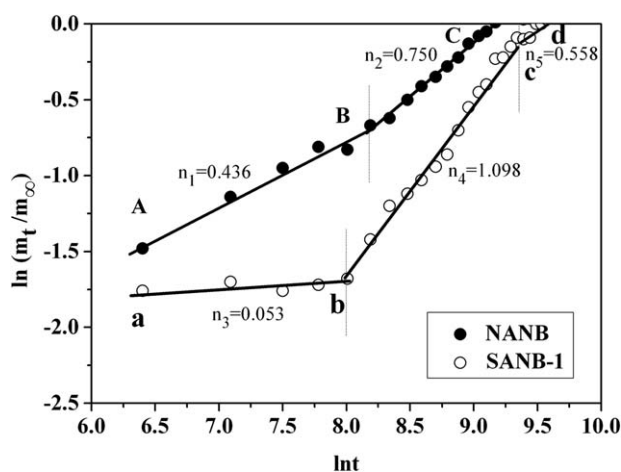


**Figure 10** Plots of  $\ln(M_t/M_\infty)$  versus  $\ln t$  for NANB and SANB-1.



were attributed to the physical entanglement interactions between PAANa long chains and the Ca-alginate gel networks. The compact structure could prevent the release medium from permeating into the hydrogel beads, and therefore, the swelling and drug-release rates from SANB-1 and SANB-2 decreased obviously. Hence, the dual-responsive SANB could be exploited to develop an excellent drug-delivery device with sustained release characteristics.

## References

1. Shi, J.; Alves, N. M.; Mano, J. F. *Adv Funct Mater* 2007, 17, 3312.
2. Ju, H. K.; Kim, S. Y.; Lee, Y. M. *Polymer* 2001, 42, 6851.
3. Park, T. G. *Biomaterials* 1999, 20, 517.
4. Gutowska, A.; Seok Bark, J.; Chan Kwon, I.; Han Bae, Y.; Cha, Y.; Wan Kim, S. *J Controlled Release* 1997, 48, 141.
5. Schield, H. G. *Prog Polym Sci* 1992, 17, 163.
6. George, M.; Abraham, T. E. *J Controlled Release* 2006, 114, 1.
7. Collins, M. N.; Birkinshaw, C. *J Appl Polym Sci* 2008, 109, 923.
8. De Moura, M. R.; Guilherme, M. R.; Campese, G. M.; Radovanovic, E.; Rubira, A. F.; Muniz, E. C. *Eur Polym J* 2005, 41, 2845.
9. Guo, B. L.; Gao, Q. Y. *Carbohydr Res* 2007, 342, 2416.
10. Shi, J.; Liu, L. H.; Sun, X. M.; Cao, S. K.; Mano, J. F. *Macromol Biosci* 2008, 8, 260.
11. Hutchens, S. A.; Benson, R. S.; Evans, B. R.; O'Neill, H. M.; Rawn, C. J. *Biomaterials* 2006, 27, 4661.
12. Weng, L. H.; Gouldstone, A.; Wu, Y. H.; Chen, W. L. *Biomaterials* 2008, 29, 2153.
13. Milosavljević, N. B.; Kljajević, L. M.; Popović, I. G.; Filipović, J. M.; Kalagasidis Krušić, M. T. *Polym Int* 2010, 5, 686.
14. Şanlı, O.; Kondolot Solak, E. *J Appl Polym Sci* 2009, 112, 2057.
15. Mathews, D. T.; Birney, Y. A.; Cahill, P. A.; McGuinness, G. B. *J Appl Polym Sci* 2008, 109, 1129.
16. Wang, Q.; Dong, Z. F.; Du, Y. M.; Kennedy, J. F. *Carbohydr Polym* 2007, 69, 336.
17. Zeng, M. F.; Fang, Z. P.; Xu, C. W. *J Appl Polym Sci* 2003, 91, 2840.
18. Yuk, S. H.; Cho, S. H.; Lee, H. B. *Pharm Technol* 1992, 9, 955.
19. Kokue, E. I.; Takahashi, Y. J. *Jpn J Pharmacol* 1976, 26, 760.
20. Adams, D. J.; Weaver, D. W.; Wilber, W. R.; Guo, J. H.; Greenberg, E. S. U.S. Pat. Appl. 20030187167 (2003).
21. Shi, J.; Liu, L. H.; Liu, X. P.; Sun, X. M.; Cao, S. K. *Polym Adv Technol* 2008, 19, 1471.
22. Hoya, W. T.; Omiya, E. A.; Soka, K. Y.; Yono, T. T.; Sayama, H. N. U.S. Pat. 4,059,686 (1977).
23. Kim, J. H.; Lee, S. B.; Kim, S. J.; Lee, Y. M. *Polymer* 2002, 43, 7549.
24. Verestiuc, L.; Ivanov, C.; Barbu, E.; Tsibouklis, J. *Int J Phytorem* 2004, 269, 185.
25. Rokhade, A. P.; Shelke, N. B.; Patil, S. A.; Aminabhavi, T. M. *Carbohydr Polym* 2007, 69, 678.
26. Shi, J.; Alves, N. M.; Mano, J. F. *Macromol Biosci* 2006, 6, 358.
27. Arco, M. D.; Cebadera, E.; Gutiérrez, S.; Martín, C.; Montero, M. J.; Rives, V.; Rocha, J.; Sevilla, M. A. *J Pharm Sci* 2004, 93, 1649.
28. Grech, J. M. R.; Mano, J. F.; Reis, R. L. *J Mater Sci Mater Med* 2010, 21, 1855.
29. Orive, G.; Hernández, R. M.; Gascón, A. R.; Lgartua, M.; Rojas, A.; Pedraz, J. L. *Biotechnol Bioeng* 2001, 76, 285.
30. Gil, E. S.; Hudson, S. M. *Prog Polym Sci* 2004, 29, 1173.
31. Muniz, E. C.; Geuskens, G. *Macromolecules* 2001, 34, 4480.
32. Soppimath, K. S.; Aminabhavi, T. M.; Dave, A. M.; Kumbar, S. G.; Rudzinski, W. E. *Drug Dev Ind Pharm* 2002, 28, 957.
33. Ritger, P. L.; Peppas, N. A. *J Controlled Release* 1987, 5, 37.
34. Reddy, K. M.; Babu, V. R.; Rao, K. S. V. K.; Subha, M. C. S.; Rao, K. C.; Sairam, M.; Aminabhavi, T. M. *J Appl Polym Sci* 2008, 107, 2820.